



Project of Strategic Interest NEXTDATA

Deliverables D1.4.2-D1.4.3 Report on measurement activities; data transmission to the archives and the General Portal

WP Coordinator: Valter Maggi
DISAT-UNIMIB, Bologna

Authors:

V.Maggi, M. Moretti, M. de Amicis
DISAT-UNIMIB, Bologna

C. Ravazzi, R. Pini
IDPA-CNR

L. Castellano
DISAT-UNIMIB

M. Potenza, F. Cavaliere
FISICA-UNIMI

R. Colucci
ISMAR-CNR

C. Mayer, A. Lambrecht
BAW-Germany

D. Bernasconi, L. Bonetti
EvK2CNR

C. Smiraglia, G. Diolaiuti
DISTER-UNIM

Mineral dust on the Colle del Lys (Monte Rosa, Italy)

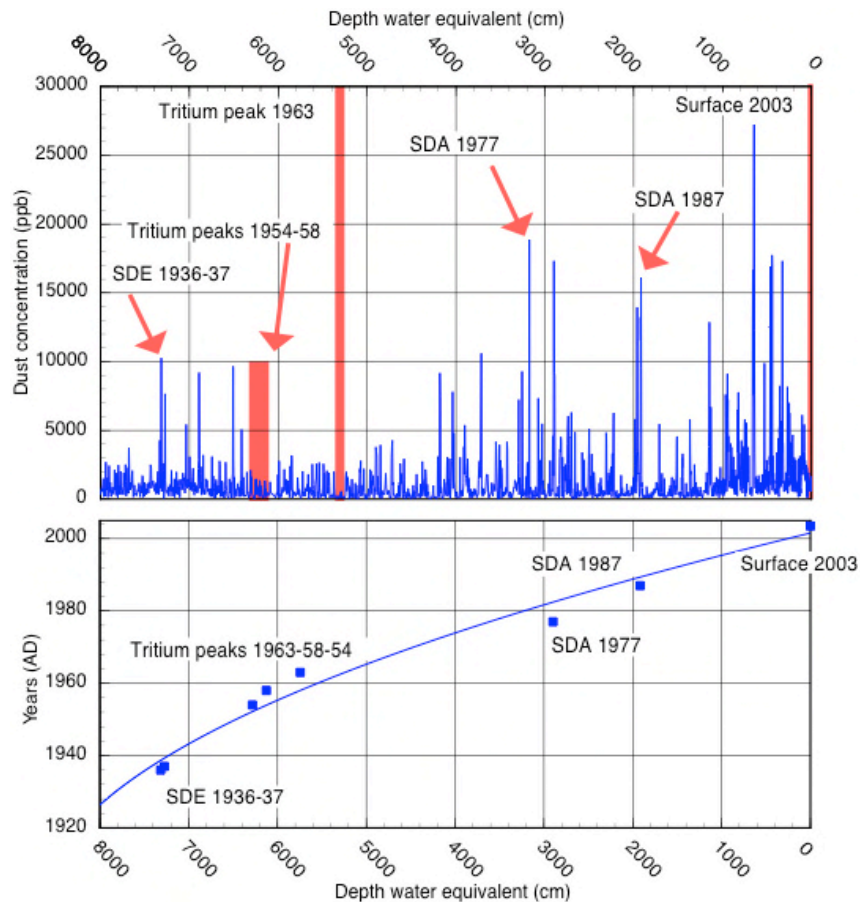


Fig. 1. Cd103/1 depth-age relationship

The dust record of CDL03/1, drilled in 2003 at Colle del Lys (Monte Rosa, Italian Alps) is characterised by a background signal of 20-500 ppb, with huge peaks that can reach 20 ppm or higher (Fig. 1). Moreover, some of these peaks can reach a concentration which is high enough to become visible, with colours from light yellow to light brown. All these peaks, recognized as Saharan Dust Events (hereafter SDE), are generally associated with long-range transport from North African deserts, controlled by atmospheric pressure fields in the Mediterranean area or the Atlantic Ocean, and by the amount of suspended material blown-up by the wind (Maggi et al., 2006; Barkan et al., 2005; Rogora et al., 2004; Wagenbach, 1989; Wagenbach et al., 1996). Although significant variability of dust concentrations was observed, it is not easy to define a systematic seasonality of events to be used in dating the ice core (Fig. 1). Actually, the low contents of dust during Winter and the summer dust increases can be influenced by different processes: 1) high concentration of Saharan dust reaching the Alps disturbing the background signal, 2) snow accumulation variability changing the dust concentration on the glaciers, 3) dust transport from regional and local sources, strongly related to moisture conditions (more or less humid) in the region of emission, 4) variability of dust source regions. However, by using a provisional time-scale based on reference horizons in the ice, we extrapolated the depth/age relationship, dating the entire record year by year (Fig. 2). The comparison between the ^{137}Cs activity peaks and the Megatons per years estimate due to the atmospheric nuclear test explosions (Tretyak and Zdesenko, 2002),

permits to better define the depth/age relationship of the ice core (Clemenza et al., 2012).

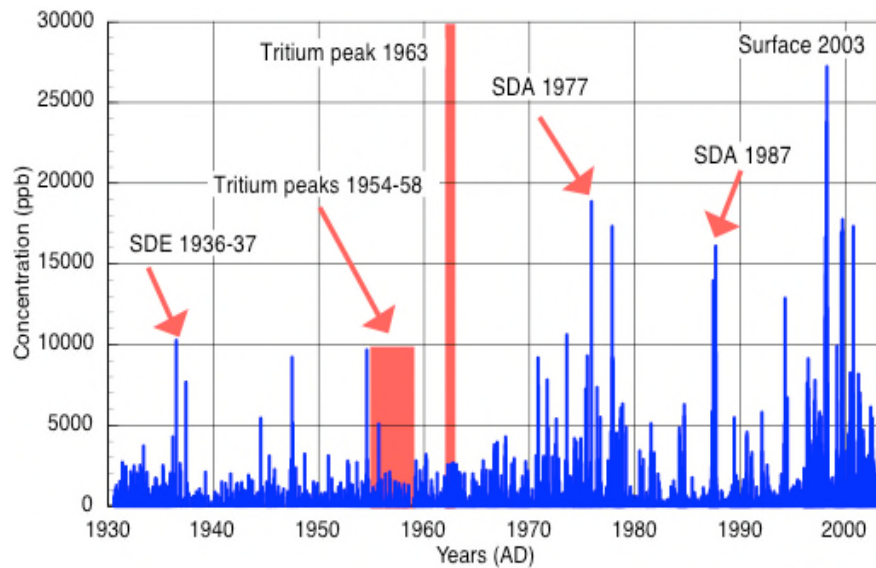


Fig. 2 – The Cd103/1 dust record in age scale.

The CDL03/1 dust record shows two main periods with high dust concentration, and two periods with lower dust peaks. From the '30s to around 1970, the background concentration reaches 2 ppm, with some spikes of 10 ppm at maximum. Two visible layers at 72 m depth, a few cm apart, are observed: they are related to strong dust events which occurred on 1936-37 (Wagenbach et al., 1989). For the upper 40 m no other visible layers were observed, and only few spikes can be related to Saharan events. From 1970 to 1980 the background dust concentration was characterised by values of about 3 ppm, with the appearance of a seasonal cycle (fig. 3). In this period, the well-known 1977 dust layer (with a dust concentration exceeding 15 ppb, 20 cm wide) was identified (Maggi et al., 2006; Wagenbach, 1989). All other peaks show dust concentrations lower than 10 ppm, without a clear seasonality. The following portion of the record, from the '80s to 1996, seems to be characterized by a decrease in the average dust concentration, with a background mean value of about 1 ppm, and a clearer seasonality, probably related to an increase of the accumulation rate (fig. 3). For the upper part of the ice core, until 2003, the peak dust concentration increased again (reaching 25 ppm with the appearance of more and more visible layers).

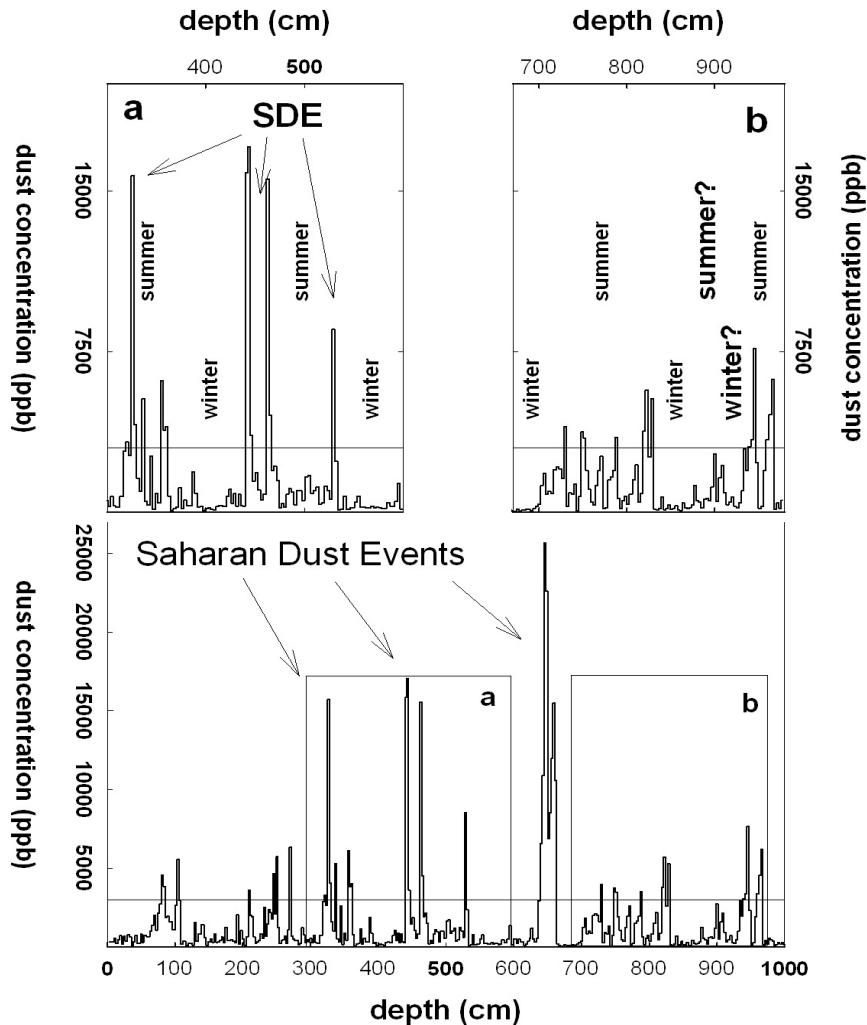


Fig. 3. Seasonality in the mineral dust record identified by background and Sahara dust events in the CDL03/1 record.

The minimum dust concentrations, observed in the CDL03/1, are considered to be representative of the background values, and were generally ascribed to winter periods, when the strong atmospheric stratification inhibits the vertical transport of mineral dust from the Earth's surface to high mountain regions, thus limiting the direct transport from regional source areas (i.e. central Europe, northern Italy, eastern Europe), see for instance Prunkert et al. (2001, 2003). The highest dust concentration, about 2-5 times larger than the background values, can be related to enhanced vertical air-mass transport in summer, allowing the arrival of dust from the continental areas of Europe. The observed variability in dust concentrations within the ice core appears to be not related with a variability in the size distribution. Indeed, it should be noted that the mode of the size distribution of background dust is very similar to that observed in central Antarctic glaciers (i.e. Dome C, East Antarctic plateau, 3300 m a.s.l.), whose source areas lie at distances of 6-8000 km (i.e. South America, Australia) (Delmonte et al., 2002, 2003). This suggests that the dust of the core CDL03/1, when present at low concentrations, is well representative of the global background values.

The dust background size distribution showed a size distribution with mode at about 1.5 μm - 2.0 μm . Although this modal range is quite wide, due mainly to the low dust concentration, these values are similar to average values observed in ice cores from polar regions, where fine dust fallout is solely controlled by the general circulation (Steffensen et al., 1997; Delmonte et

al., 2003). The size distribution curves of the two levels of fine dust used as reference horizons for dating are different, with distinct modes shifted to much higher values. Indeed, the Visible Saharan dust Event (VSE) recorded in 1977 shows a volume distribution with a much higher concentration and greater symmetry. Furthermore, the mode is shifted towards larger diameters, with average values of about 5.0 μm . Although this principal mode is particularly high, this size distribution is not so far from average size distributions of atmospheric dust, suggesting long-range atmospheric transport (Pye, 1987). The 1987 dust event has a slightly lower mode of about 4.0 μm , with a long tail towards particles with smaller diameters. This feature is different from all other size distribution measurements, which are more symmetric. Indeed, although the log-normal distribution fits very well with the data, it differs greatly from its normally much more symmetric distribution (Pye, 1987). The 1987 VSE shows a log-normal size distribution with a maximum diameter at around 7 μm , and therefore presents the same dimensional classes as the background. The 1977 event, instead, shows particles diameters range up to 20.0 μm , with the maximum concentration of all CDL03/1 dust records.

Even if the CDL03/1 ice core is not a complete record of all the dust transport events from North Africa to the Alps, however it represents a valuable source of information concerning this class of events. On average, SDE events determine both higher dust concentrations and a modal shift towards larger diameters (i.e. the 1977 VSE, which shows mode values of around 5.0 μm). There are no specific works on this particular aspect of atmospheric dust transport, but one of the factors producing a less efficient particle selection is probably the lack of, or a significant decrease in, precipitation along the air-masstrajjectory, thereby reducing atmospheric scavenging.

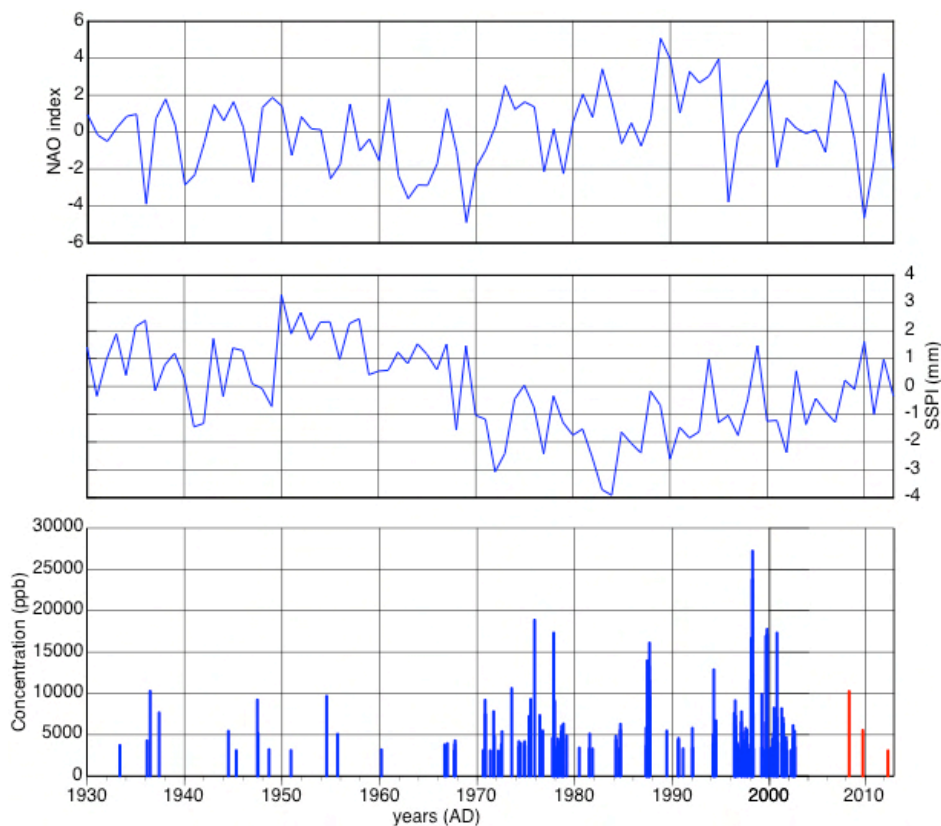


Fig. 4. NAO index, Sahel Standardized Precipitation Index, and Saharan dust events in CdL03/01 (blue) and CDL12/1 (red) (more than 3000 ppb concentration).

Prospero & Lamb (2004) highlight how the solid atmospheric load over the Barbados increased in the May-September period from the late '60s until the early '80s, and then remained constant for the following 20 years. This record shows a strong anti-correlation with precipitation anomalies in the area of the Sahel (SSPI index), which therefore links the increase in the solid atmospheric load over the tropical Atlantic north of the Equator with a general decrease in precipitation in the African area. The dust record at Colle del Lys also reveals an increase in concentration starting in the late '60s, particularly of Saharan events. Although it is impossible to establish the seasonal chronology of these peaks, the main North African dust events generally occur in the spring-summer period (Wagenbach, 1989; Prospero & Lamb, 2004). Although a not-negligible variability affects the dust concentration and the frequency of Saharan dust events, the CDL03/1 dust record shows high concentrations through to the '90s (Fig. 4).

We investigated the possible correlation between the occurrences of SDEs (as deduced by the analysis of dust deposition in the ice core) with the variability of the North Atlantic Oscillation (NAO), which concurs in determining the storm track position in the Mediterranean-European area. The general positive trend of the NAO index appears to be related with the occurrence of the dust events identified by the analysis of the CDL03/1 record (Fig. 4). Transport from North Africa is not controlled only by the relative position of cyclones and anticyclones, but also by their intensity. This is essential because atmospheric dust must first be injected into the system of cyclonic circulations, which distributes it along its trajectory. The two opposing Azores high and Icelandic low pressure centres not only control the trajectory of cyclones and therefore very long-range transport, but possibly also turbulence over North Africa, which determines the injection of dust into the atmosphere. Furthermore, the NAO controls the transit of cyclones over the Mediterranean area and the frequency of dust transport towards the Alps. The observed similarity between the CDL03/1 dust record and the Barbados record (Prospero & Lamb, 2004) indicates that there is a relationship between events in the Sahel, possibly correlated to Indian monsoons, and events in the Mediterranean area. Records of insoluble atmospheric dust can be important instruments for climate studies, especially in areas like the Mediterranean, where traditional chemical records are influenced by strong anthropogenic inputs. Because the record of CDL12/1 until now do not reach the top of CDL03/1, it cannot be compared with NAO and SSPI indices. However, is clear that in the last 6 years, 2006-2012, the Saharan events at Colle del Lys are less concentrated, and with lower spike frequencies with respect to the six years 1997-2003 (top of CDL02/1).

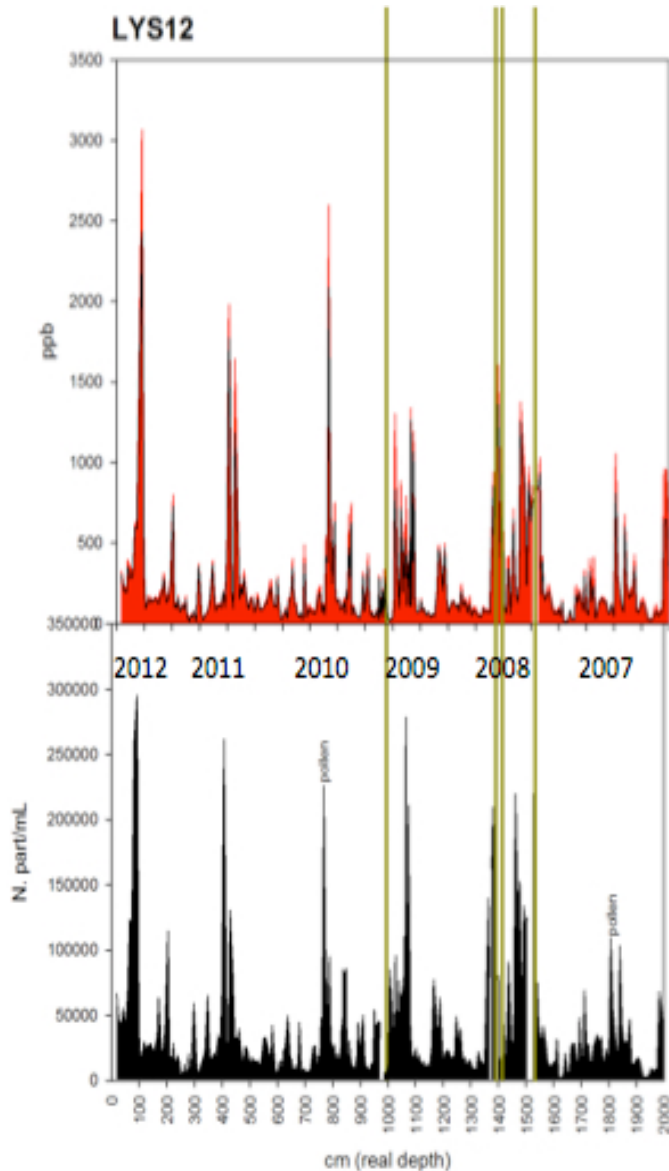


Fig. 5. CDL12/1 mineral dust record, in mass (ppb, red) and number (part/mL, black) with the visible layers (brown lines), and indication of where pollen particles were observed by scanning electronic microscope imaging.

Figure 5 shows the measurements of mineral dust concentration in the first 20 m of the 2012 Colle del Lys ice core (CDL12/1). A first important result is related to the strong seasonality observed, that allows to improve the dating procedure of the entire ice core and to provide a more reliable correlation with the previous mineral dust records from the same site. The 400 samples show concentrations between 10-50 ppb at the background level, reaching values up to 3 ppm during the concentrated spikes. Very high concentration events, reaching 10 ppm, were easily observed on the ice core surface due to the red-yellow-brownish colour dust. The low concentration periods were related to winter time transport, high-concentration spikes were related to spring-summer periods when transport of mineral dust from North Africa to the Alpine area took place (Saharan events, Maggi et al., 2006). Figure 5 includes a preliminary dating of the annual counts (number of particles concentration: N/mL - in black) and mass concentration (ppb: in red), both obtained by Beckmann-Coulter 3© instrument. The mass was calculated by assuming a spherical particle shape and using a mean mineral density of 2.6 g/cm^3 (Delmonte et al. 2002; Maggi et al., 2006). The light-brown lines in figure

1 represent the visible layers observed on the ice core, and because of their very high concentration, these spikes are not shown in the plot. Scanning Electronic Microscope (SEM) observations show the presence of pollen remains in some samples, which will be studied to improve the knowledge of the source areas.

Application of minimal models to understand glacier retreat: the example of Careser Glacier, Ortles-Cevedale, Italy.

Alpine glaciers respond rapidly and strongly to climatic and environmental modifications (UN A/Res/62/196).

The development of theoretical work on glaciers advance or retreat needs the definition of mathematical and numerical models to assess glacier response to climate change scenarios.

The behaviour of a valley glacier is determined by the sum of accumulation and ablation, which constitute its mass balance. These processes depend on several factors: climatic conditions, topographic setting, geographic position and ice mechanics.

Mathematical models try to reduce this complex situation to a simple description, based on the laws of physics, that represents the starting point for the numerical algorithms. The models can range from simple to very complex, with few to many degrees of freedom respectively.

It is interesting to note that, sometimes, even if the models become more and more complex, the understanding of the mechanisms under study does not improve. So the use of simple models can often help to achieve understanding and verify the dynamical behaviour of glaciers. A type of simple model is called the "Minimal Glacier Model" (Oerlemans, 2011). The term minimal glacier model indicates a class of models that does not explicitly describe how quantities like ice thickness, basal water pressure, sliding velocity and others vary in space. A simple diagnostic relationship between glacier length and average thickness is adopted, using perfect plasticity assumption, and the only dynamical variable of the model is the glacier length L . As in glacier models with spatial resolution and more complex structure, the evolution of the glacier is calculated from an integrated continuity equation.

This following work focuses on Ortles-Cevedale group, in the Eastern Italian Alps, in particular in this study the minimal model is applied to the Careser glacier.

Study region and data set

The Careser glacier (Vedretta del Careser) is located on the right side of Val di Peio, called Val de la Mare, Eastern Italian Alps (Figure 6). The catchment lies in the southern part of the Ortles-Cevedale massif, and forms the artificial lake Careser. At the end this catchment generates the Noce river. The Careser glacier begins from the pass between Marmotta peak (3330 m a.s.l.) and the Tre Venezie peaks (3386 m a.s.l., 3371 m a.s.l. and 3356 m a.s.l.).

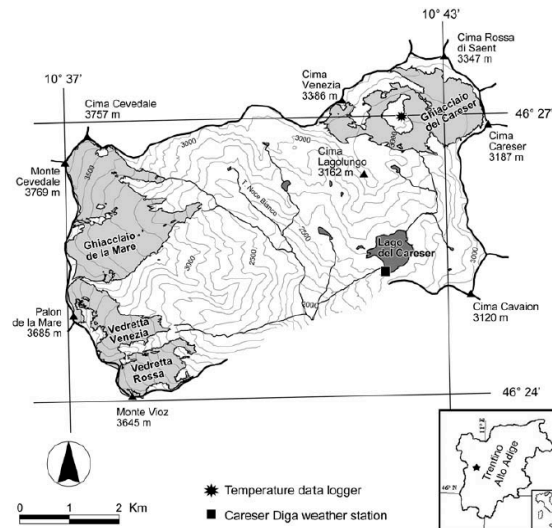


Fig. 6. Geographical setting of Careser Glacier in Val de la Mare, Pejo (TN).

Two weather stations have operated since the 1920s in Val de la Mare: Careser Diga (2605m a.s.l.) and Cogolo (1200 m a.s.l.), recording 2m air temperature and precipitation. In front of the Careser, there is another glacier, called Vedretta de La Mare, which is very different from the first one: Careser (2870 – 3279m a.s.l.) is flat and mainly exposed to the South, instead La Mare (2650 – 3769m a.s.l.) is steeper and exposed to the East. Today the mass balance is negative for both glaciers and the two ice bodies show retreat, but La Mare glacier still has an accumulation area, while Careser has no positive accumulation and exhibits a rapid mass loss (Zanon, 1982; Carturan and Seppi, 2007, 2009; Carturan et al., 2012, Carturan et al., 2013).

The Careser glacier is the residual accumulation area of a much wider glacier which during the Little Ice Age, exhibited a well developed valley tongue.

On Careser, mass-balance and ELA (Equilibrium Line Altitude) measurements have been carried out since 1967 and the data series, the longest for the Italian Alps, extends until present without interruption (Zanon, 1982; Carturan and Seppi, 2007; Carturan et al., 2009a).

The strongly negative mass balances result in huge morphological changes and positive feedbacks contribute to accelerate the ablation process and fragmentation of ice body: in 2012, 90% of total area of glacier survives in the eastern part of Careser (Figure 7). From 1981 the ELA was normally above the highest elevation of the glacier, with only a few exceptions when the Accumulation-to-Ablation Ratio was zero or near-zero (max value 0.14 in 1993) (Figure 8). Today the Careser glacier has no accumulation area and its complete extinction is expected within a few decades.



Fig. 7. Eastern part of Careser glacier; today representing the 90% of the total area.

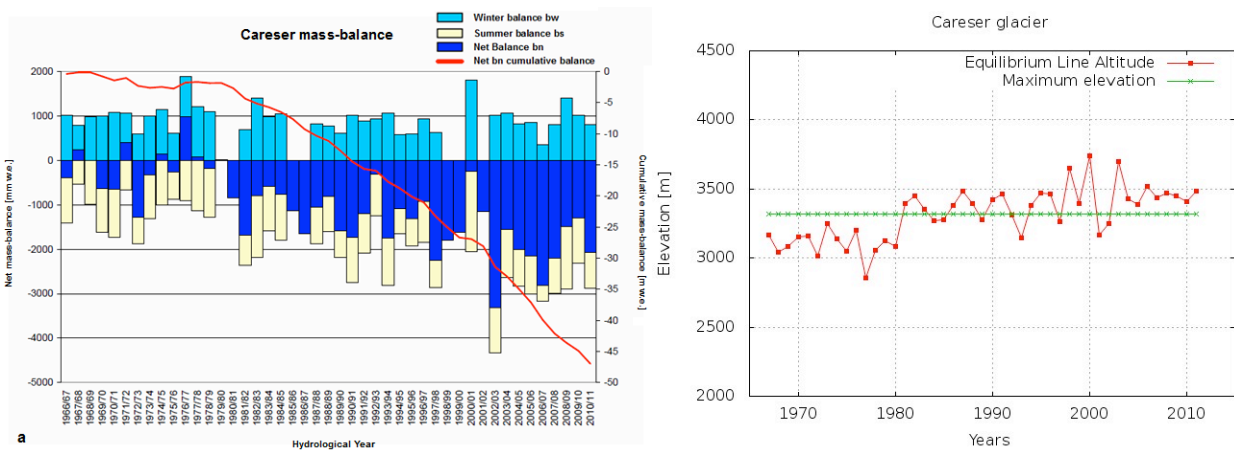


Fig. 8. Historical data set of Careser glacier: (a) cumulative and net seasonal mass balance; (b) Equilibrium Line Altitude compared with the maximum elevation of the glacier.

Minimal Glacier Model

The Minimal Glacier Model is based on the equation:

$$\frac{dV}{dt} = B_s + F \quad (1)$$

where V is the total ice volume, B_s is the total surface balance rate and F is the calving flux, which is zero in valley glacier. The glacier volume V is given by the product of the mean ice thickness H_m and the glacier length L .

Since the width W is assumed constant along the glacier, volume changes are determined by length changes. Therefore volume changes can be expressed as:

$$\frac{dV}{dt} = \frac{d}{dt}(WH_mL) = W \left(H_m \frac{dL}{dt} + L \frac{dH_m}{dt} \right) \quad (2)$$

where H_m can be defined by:

$$H_m = \frac{1}{L} \int_0^L H dx \quad (3)$$

The value of mean ice thickness can be related to the slope of the ice bed by using perfect plasticity in a global sense, a first order estimate of how the thickness of a glacier varies with its horizontal dimension.

This theory considers the condition that the shear stress at the base of a glacier cannot exceed a threshold yield stress τ_0 , given by

$$\tau_0 = \rho g H \left| \frac{dh}{dx} \right| = \rho g H_m s \quad (4)$$

where the stress is related to the ice density ρ , gravity acceleration g , surface elevation h and bed slope s .

Extensive experimentation with numerical glacier models to define the expression of H_m , shows that H_m depends also on L^k , where k varies from 0.40 to 0.45, depending on the bed slope (Oerlemans, 2011). The larger values of k are for smaller slopes of the bed. Then, the exponent 0.5 is a workable approximation in perfect plasticity principle.

A meaningful expression for H_m is (Oerlemans, 2011):

$$H_m = \frac{\alpha_m}{1 + \nu s} L^{1/2} \quad (5)$$

where \bar{s} is the mean bed slope over the glacier length and α_m and ν are constants. If the bed slope is set to zero, the mean thickness varies with the square root of the glacier length, which is in agreement with perfectly plastic behaviour.

From the above expressions one obtains the evolution equation for the glacier length:

$$\frac{dL}{dt} = \left(\frac{3\alpha_m}{2(1 + \nu s)} L^{1/2} - \frac{\alpha_m \nu}{(1 + \nu s)^2} L^{3/2} \frac{\partial \bar{s}}{\partial L} \right)^{-1} \frac{B_s}{W} \quad (6)$$

Considering a linear profile, the surface balance B_s is given by:

$$B_s = W \beta \int_0^L (H(x) + b(x) - E) dx = (H_m + \bar{b} - E) \beta W \quad (7)$$

where \bar{b} is the mean bed elevation, E is the ELA and b is the mass balance gradient along the glacier.

A simple representation of the bed $b(x)$, useful for Careser, is a simple concave bed, given by:

$$b(x) = b_0 e^{-x/x_1} = b_0 - sL \quad (8)$$

where b_0 is the maximum elevation of glacier's head and x_l is the length scale that determines how quickly the height of the bed decreases:

$$x_l = -\frac{L}{\ln\left(1 - \frac{sL}{b_0}\right)} \quad (9)$$

From this one obtains:

$$\frac{\partial \bar{s}}{\partial L} = -\frac{b_0\left(1 - e^{-L/x_l}\right)}{L^2} + \frac{b_0 x_l^{-1} e^{-L/x_l}}{L} \quad (10)$$

Model set up

For Careser Glacier there are several maps and cartographic and geomorphological studies. The consequence is the existence of DEMs (Digital Elevation Model), built using data collected by remote sensing techniques and from land surveying from 1933. The last is a DEM with resolution 2mx2m, derived from a Lidar aerial survey in 2007 (Carturan et al., 2013).

Using DEMs, Carturan et al. reconstructed the evolution of polygons, contour maps and dimension of the glacier. The flow line drawn in Figure 9 follows the accumulation-ablation dynamics and it is created from DEM analysis of elevation and slope. The Minimal Glacier Model is applied along this flow line.

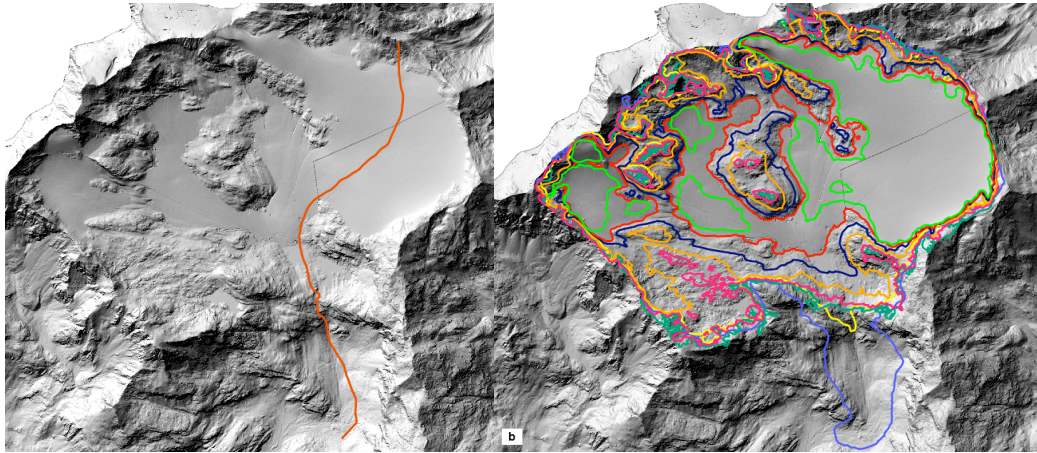


Fig. 9. DEM analysis of the Careser glacier (Carturan et al., 2013): (a) flow line obtained from contour lines; (b) different polygons of the outer glacier limit, in different years starting from 1933.

Model parameters

Only the ν parameter is chosen a priori as $\nu=10$ (Oerlemans, 2011). The other constants for Careser Glacier are: $s = 0.16$, $b_0 = 3320\text{m}$. The parameter a_m is estimated from the length and mass balance data.

Meteorological data

In the minimal model, the input data are given by the mass balance gradient along the glacier, b , and the Equilibrium Line Altitude, E .

The mass balance gradient depends on the net mass balance \dot{b} following the relations

$$\beta = \frac{d\dot{b}}{dz} = \frac{\dot{b}}{\bar{h} - E} \quad (11)$$

where dz is the altitude variation and \bar{h} is the mean elevation

$$\bar{h} = \bar{H} + b_0 - \frac{L \cdot s}{2} \quad (12)$$

with \bar{H} mean thickness of the glacier.

\dot{b} and E are closely related to climate forcing, particularly winter precipitation and summer air temperature. Variations can therefore commonly be attributed to changes in these two variables. In order to relate the glacier parameters to climate, both series of measured weather values are required.

Glacier snout variations respond to climatic fluctuations with a time delay from years to tens of years (Oerlemans, 2001). Studying the correlations between climatic variables and snout fluctuations of the glaciers, Bonanno et al., 2013 found that best correlations are found with

- winter precipitation from December to March;
- summer temperature from June to September.
-

The winter precipitation and summer air temperature have been related to the mass balance series using a bivariate fit:

$$\dot{b}_i = aT_{s,i} + bP_{w,i} + c \quad (13)$$

where i represents the i -th year, $T_{s,i}$ is the summer 2m air temperature and $P_{w,i}$ is the winter precipitation for the same year.

The ELA is related to the climatic variables through:

$$E_i = uT_{s,i} + vP_{w,i} + z \quad (14)$$

To obtain the relationship between glacier behaviour and climate fluctuations, it is used the ERA-Interim data set, a global atmospheric reanalysis produced by the European Centre for Medium-Range Weather Forecast (ECMWF). ERA-Interim analysis daily products, from 1 Jan 1979, are publicly available on the ECMWF Data Server, at 1.5° resolution, and can be obtained at 0.75° resolution (Dee and others, 2011).

The calculated values of those bivariate fits, eq. (13) and (14), using ERA-Interim summer temperatures and winter precipitations, are:

\dot{b}_i coefficients	E_i coefficients
$a = -0.67$	$u = 113.2$
$b = 4.99$	$v = -795.8$

$c = 5.14$	$z = 2279.7$
Fitting coefficient R	
$R_b = 0.73$	$R_E = 0.68$

Tab. 1. Values of bivariate fits and fitting coefficients for net mass balance and ELA analysis.

The resulting \hat{b}_i fit is shown in Figure 10, showing good match between the measured net mass balance and the fitted values from climate variables.

The available ELA fit is reported in Figure 11, proving the accuracy of this evaluation.

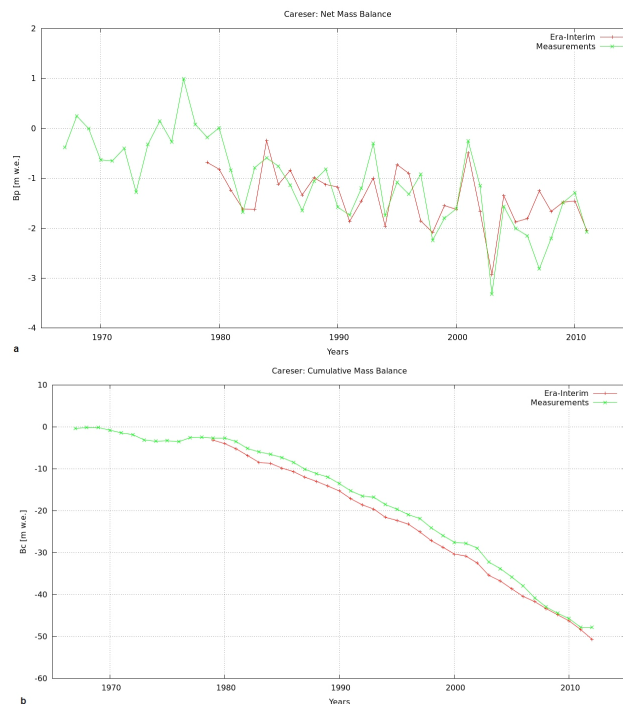


Fig. 10. Measured mass balance (green) compared with the calculated mass balance (red) from climate data provided by Era-Interim: (a) annual net mass balance; (b) annual cumulative mass balance, since 1979.

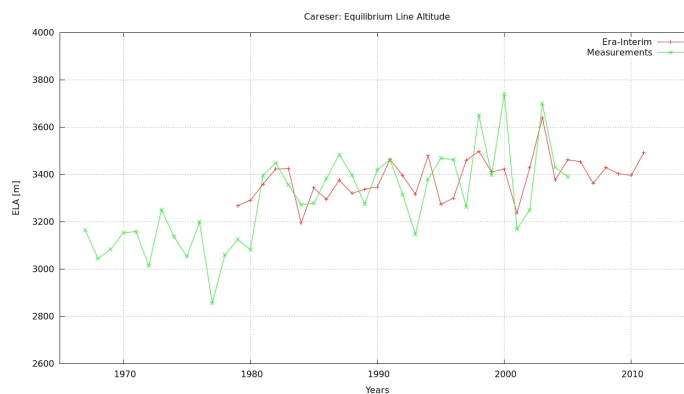


Fig. 11. Estimated Equilibrium Line Altitude (green) compared with the calculated Equilibrium Line Altitude (red) from climate data extracted from Era-Interim.

In future work, these validated input data will be used to forecast the evolution of the Careser glacier, using future weather conditions extracted from global climatic scenarios.

Results

The measurement of the length variations of Careser glacier begins in 1933 with the oldest DEMs acquired by topographic map, but the mass balance and ELA records are available since 1967, while the climatic series from ERA-Interim span the period from 1979 to 2013.

The simulated results with different input series (in-situ observations or ERA-interim driven glacier values) are shown in Figure 12. The comparison illustrates a good match between length variations obtained with mass balance and ELA, and the results obtained by parameterizing the mass balance and the ELA variations from climate data, supporting the use of the bivariate fit technique.

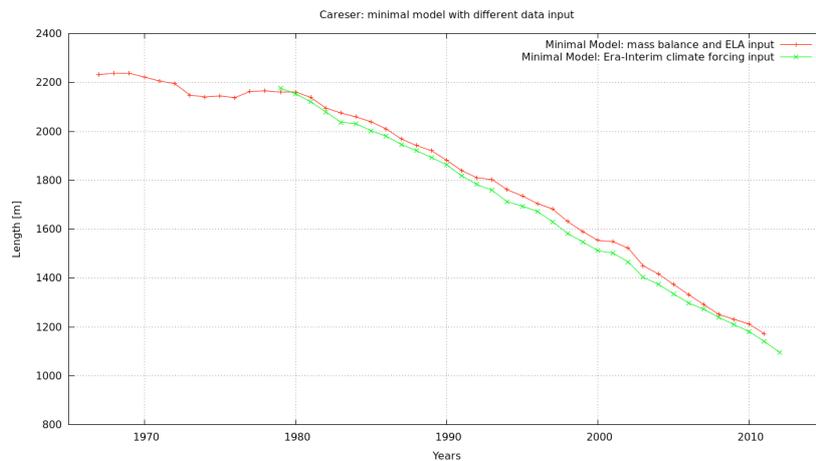
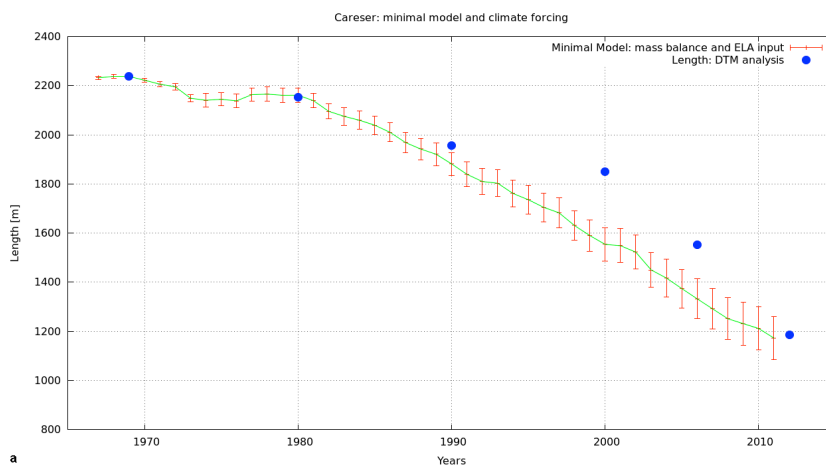


Fig. 12. Minimal model results: comparison between model results obtained with measured glacier mass balance and ELA (red) and results obtained by parameterizing these quantities from climate data.

Figure 13a and 13b show, however, that the minimal model does not reproduce well the measured glacier length values: the melting predicted by the model is larger than the measured one in the period 1990-2000.



a

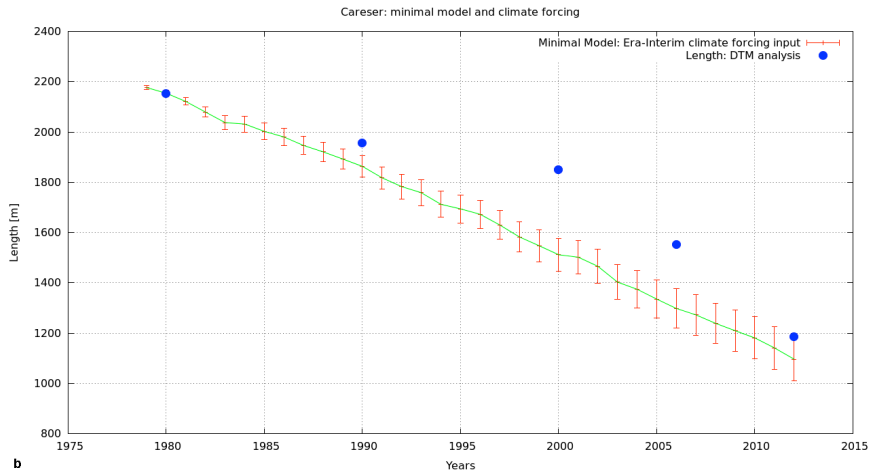


Fig. 13. Results of the different runs of Minimal Glacier Model, compared with the measured length variation: (a) results obtained using measured mass balance and ELA inputs, [1967 – 2012]; (b) results obtained using mass balance and ELA parameterized through climate data, [1979 – 2012].

The uncertainty bars are determined by the errors on the input data.

General comments

In the first paragraphs it is showed that from 1981 the Accumulation Area Ratio of Careser was always zero or near-zero. This condition stopped the ice flow and the standard dynamics of this glacier since the end of the '80s.

In the last 20 years, the Careser glacier has shown a passive melting everywhere, mostly in terms of thickness reduction, and an important disappearance of the upper part and the mid-west region. This condition makes the mid-west mass area in a complete ablation phase. When a glacier has a normal dynamical ice flow, it is characterized by two different components: the fluid dynamics of ice from the high accumulation area to the lower ablation region and the thermodynamic melting caused by the positive balance heat on the glacier surface. The balance between these processes generates the advance or retreat of the glacier, following climatic conditions.

On Careser glacier it is evident the call off of the fluid-dynamical contribution since the '80s, and an increase of the thermodynamic melting.

The break of accumulation-ablation dynamics, the rise of local melting and the drift velocity of mid-west ice reduce the speed of front retreat if we compare the real variations with model results, as shown in Figure 13. These processes create a peninsula of stationary ice, Figure 14, included and protected by two elevation drops, upwards and downwards.

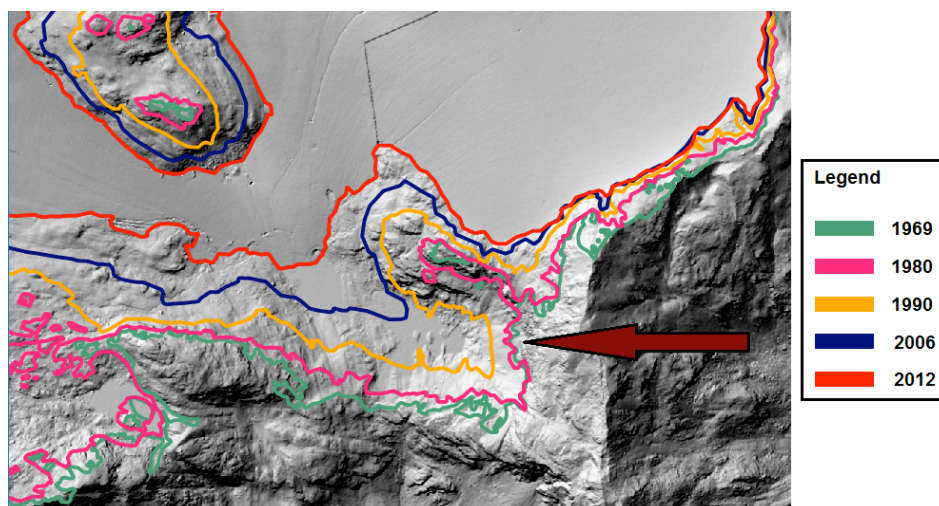


Fig. 14. Enlarged DEM view of the Careser front from 1969 to 2012: stationary peninsula.

This peninsula is a flat strip of land with slope of about 13%. At the end of this little region of about 300 m x 800 m, there is also a slight rise on the ridge of the promontory. In that area it is clear the decrease of the fluid dynamical flow of the glacier and the accumulation of drifted ice, matched with the thermodynamic melting. This situation masks the real condition of the flow line and the actual length variations of the glacier front.

Figure 15 reports the comparison between the minimal model and the results from the Linsbauer method.

At the beginning of the '80s, when the glacier started to lose mass in the northern part, the minimal model results did not match the real position of flow line and the mean thickness decreased faster than the previous years.

Afterwards, the thickness of the ice peninsula was sufficient to slow down the false front variations. Since year 2000, a change of retreat slope was evident: the ice peninsula became slim, exceeding a threshold from which the ice disappeared faster than before because of the lack of glacier mass.

The pick up of the front retreat followed the longitudinal line of the peninsula, as shown observing the polygon of glacier in Figure 14, and quickly reached the actual situation.

This event is indicated by the second point of discontinuity in Figure 15.

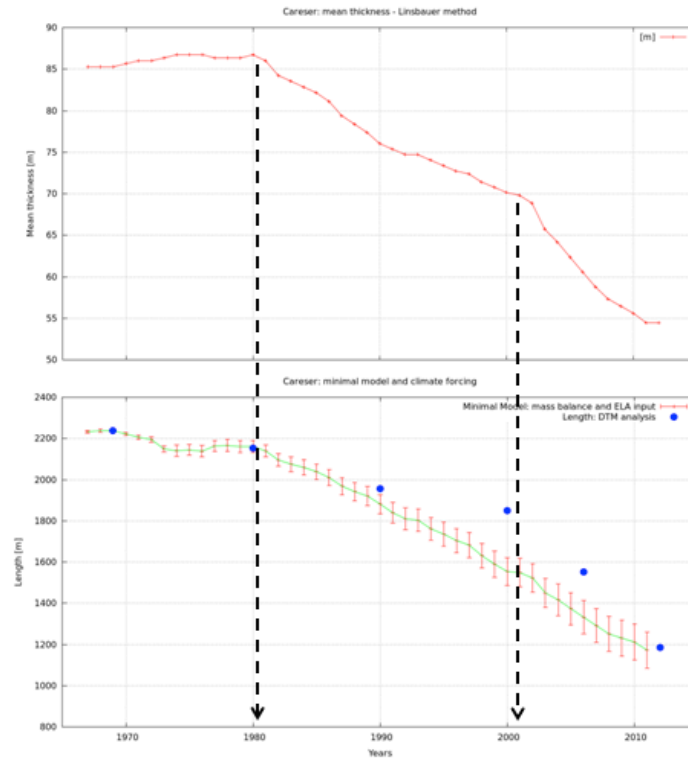


Fig.15. Trend comparison: discontinuity points in mean thickness with the Linsbauer method and front retreat with the Minimal Glacier Model.

Therefore, the physical evolution of the Careser Glacier flow line is well-explained by DEM analysis and model results, based on mechanical and dynamical principles of glaciers.

Evaluation of snow and ice depth at the accumulation area of the Baltoro-Gasherbrum Glaciers (Pakistan)

In the framework of the 2013 field expedition performed at the Baltoro Glacier (Karakoram, Pakistan) as a joint activity with the SHARE Paprika Project, some investigations were carried out in the upper glacier zone (the Gasherbrum basin) with the aim of evaluating glacier snow accumulation and of assessing glacier ice thickness.

Snow pits were dug according to the well-known protocol developed by AINEVA and ice thickness was tentatively estimated using a low frequency radar antenna (50 MHz) installed on a portable instrument (SIR 3000 - GSSI).

Snow depth at 5900 m a.s.l. resulted larger than 220 cm, with density ranging from 250 kg/m³ to 530 kg/m³.



Fig. 16. Location of one of the snow pits at the Gasherbrum basin.



Fig. 17. Performing a snow pit in the Gasherbrum basin.



Fig. 18. Fig. 2: Performing a snow pit in the Gasherbrum basin.



Fig 19. Performing radar surveys at the Gasherbrum Glacier surface.



Fig 20. Performing radar surveys at the Gasherbrum Glacier surface.

For ice thickness, two test profiles with the GSSI low frequency equipment were performed. The instrument worked well even if the setup was not optimal. The profiles show that the ice thickness is at least 300 m in the Gasherbrum area (5900 – 6000 m a.s.l.), as no bed reflection was observed. This area was investigated also to evaluate ice depth with the aim of conducting future drilling of an ice core.

For a fruitful comparison and to evaluate the reliability of the measurements, we also performed radar measurements at the Concordia site (4960 m a.s.l.). Here a short low frequency radar profile east of the weather station was made. The parallel antenna configuration was shifted between each measurement by about 2m. All measurements at on position were stacked. The result was a short (about 40 m) long profile of the base reflection which gave about 790 m of ice thickness.

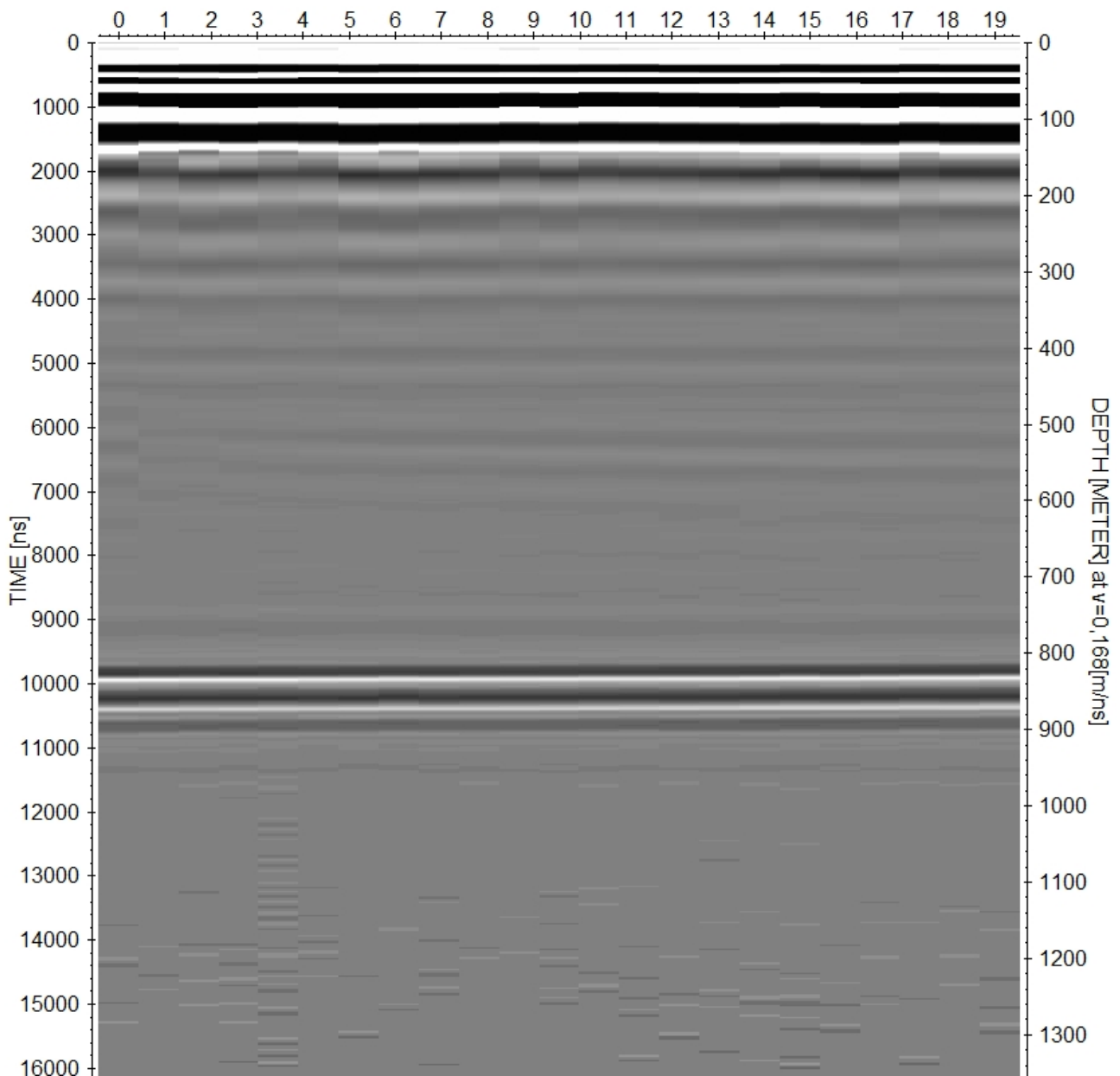


Fig. 21. Radargram showing the ice thickness at the Concordia site

This last value agrees with the one obtained for the same glacier site processing the Baltoro Glacier geometry data according to the approach introduced by Baumann and Winkler (2010), who estimated the ice depth of glaciers from the New Zealand Alps to Norway, thus suggesting a wide applicability of this approach. Application to the Baltoro Glacier data indicates for the Concordia site an ice depth ranging from 800 to 850 m.

D1.4.3: Report on technological developments.

Inflatable Tent

In the framework of a collaboration between the Earth and Environmental Sciences Dept., University of Milano Bicocca, and the Physics Dept., University of Milano, it was developed a new inflatable tent specific for polar and high mountain climatic conditions, with special emphasis on ice coring activities. The main objective is to reduce the time consumed in field camp installation. A 5m x 3m x 2.5m half-egg shaped tent, developed at the Physics Dept. of UNIMI, was inflated in less than 15 minutes without any assistance after opening. The total weight is around 80 kg with the pumps (no power generator), easily transported by helicopter, filling a large bag that can be transported by two people. The tent was tested on the roof of Physics Dept. at first, and then in the EuroCold Lab in DISAT UNIMIB at -30°C for stress tests. In October 2013, the tent was mounted and used for the Colle del Lys ice core drilling activities as a living room for 6 people for one week.

Exposed to very bad weather during that week, the tent demonstrated to be useful for this kind of activities, especially as a refuge when the wind reach 20 knots. No problems were related to the lack of a heating system, because the internal temperature did not drop below 15 degrees for the entire week. Some troubles arose for the lack of windows and ventilation holes especially during the night, when the humidity due to body transpiration condensed on the walls with some problems of dripping water inside the tent.



Fig. 22

Further development of this tent must be devoted to improving the ventilation system and reducing the total weight, also for increasing the possibility of use in more complex logistic conditions, such as remote high mountain areas (i.e Himalaya) or polar regions.



Fig. 23

Single Particle Extinction and Scattering (SPES)

A collaboration was established between UNIMIB-DISAT and UNIMI-Physics for developing a continuous measurements system for the optical properties of mineral dust trapped in glacier ice and snow. In the first year, a group of standards and samples were considered for defining the size distribution, concentration and scattering properties.

The Single Particle Extinction and Scattering (SPES) method is based upon an approach recently developed by the optics group at the University of Milan for the measurement of optical properties of single nanoparticles. It differs from the traditional optical counting methods in the experimental layout, based upon the self referenced interference of the faint scattered and the intense transmitted light. Two independent measurements are obtained for each particle, one related to the scattering cross section, the other to the extinction (scattering + absorption). In this way, the complete characterization of the optical properties is obtained as well as a superior size resolution regardless of the particle composition, shape and internal structure (which are the main limitation in traditional methods). Depending on which parameters are known from independent measurements (e.g. real or imaginary part of the refractive index, internal structure, shape, etc.), the method is capable to characterize features

beyond the limitations of traditional methods. Data are rigorously calibration free, the optical signals being constantly normalized to the instantaneous undisturbed light intensity. The method takes advantage of the high frequency sampling of the signals, which allows an accurate pulse shape analysis and makes the data analysis very robust.

An example of the typical data set is shown in Fig. 24. The two axes represent the two independent parameters (i.e. scattering and absorption), and the grey scale gives the number of events measured within each bin (white = zero, black = maximum). Data obtained from a water suspension coming from glacier ice are presented together with the expected results for perfect spheres. Numbers indicate the diameters. The two orange curves indicate the expected values for clay particles with edge-on and face-on orientation with respect to the beam direction. The departure from the scattering properties of spherical objects is evident from the broadening of the data set.

In view of the application for this project, SPES will provide a model independent characterization of the optical properties of the particles in terms of the scattering and extinction.

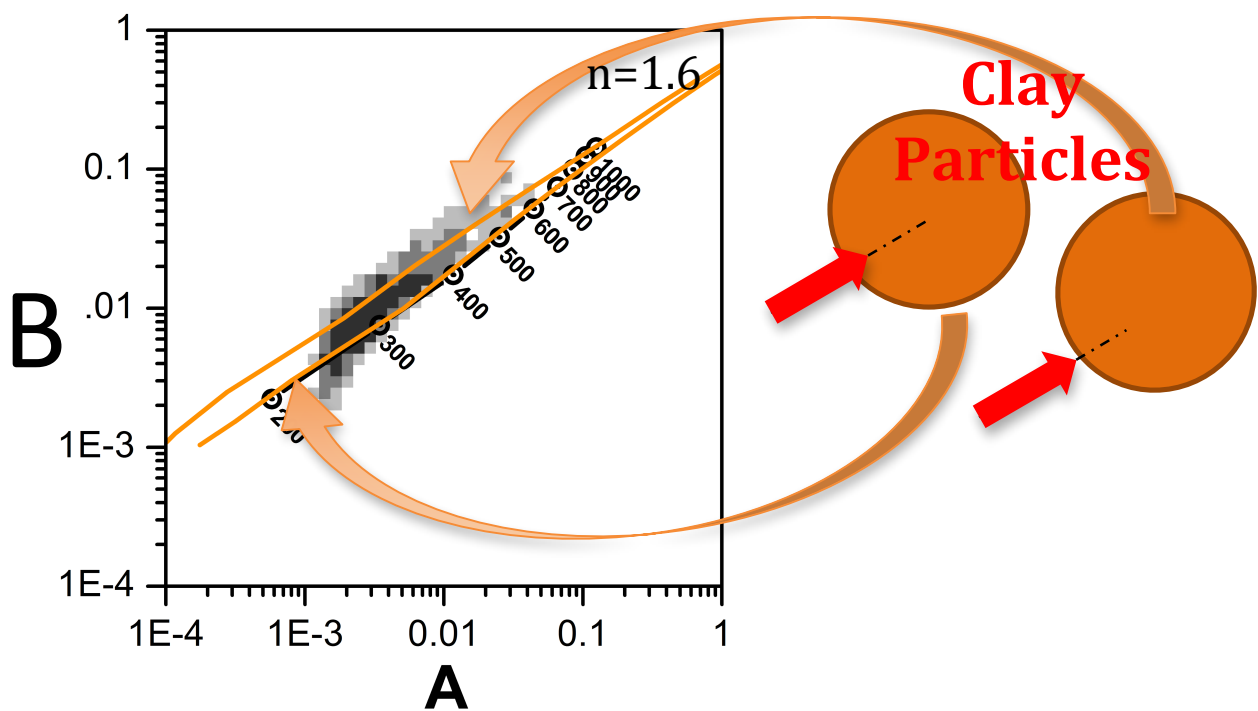


Fig. 24. Results obtained with water from glacier ice.

References

- BAUMANN S. and WINKLER S. (2010): Parameterization of glacier inventory data from Jotunheimen /Norway in comparison to the European Alps and the Southern Alps of New Zealand. *Erdkunde*, vol 64 (2), 155-177.
- BONANNO R., RONCHI C., CAGNAZZI B. and PROVENZALE A. (2013): Glacier response to current climate change and future scenarios in the northwestern Italian Alps. *Reg. Environ. Change*. v.13, n.4.
- CARTURAN L. and SEPPI R. (2007): Recent mass balance results and morphological evolution of Careser Glacier (Central Alps). *Geogr. Fis. Din. Quat.*, 30(1), 33–42.
- CARTURAN L. and SEPPI R. (2009): Comparison of current behaviour of three glaciers in western Trentino (Italian Alps). In *Epitome: Geoitalia 2009, Settimo Forum Italiano di Scienze della Terra, 9–11 September 2009, Rimini, Italy, Vol. 3*. Federazione Italiana di Scienze della Terra, 298.
- CARTURAN L., DALLA FONTANA G. and CAZORZI F. (2009a): The mass balance of La Mare Glacier (Ortles-Cevedale, Italian Alps) from 2003 to 2008. In *Epitome: Geoitalia 2009, Settimo Forum Italiano di Scienze della Terra, 9–11 September 2009, Rimini, Italy, Vol. 3*. Federazione Italiana di Scienze della Terra, 298.
- CARTURAN L., CAZORZI F. and DALLA FONTANA G. (2012): Distributed mass-balance modelling on two neighbouring glaciers in Ortles-Cevedale, Italy, from 2004 to 2009. *Journal of Glaciol.*, Vol. 58, No. 209, 2012.
- CARTURAN L., BARONI C., BECKER M., BELLIN A., CAINELLI O., CARTON A., CASAROTTO C., DALLA FONTANA G., GODIO A., MARTINELLI T., SALVATORE M.C. and SEPPI R. (2013): Decay of a long-termmonitoredglacier: Careser Glacier (Ortles-Cevedale, EuropeanAlps). *The Cryosphere.*, 7, 1819-1838,2013
- CLEMENZA, M., CUCCIATI, G., MAGGI, V., PATTAVINA, L. and PREVITALI, E., 2012: Radioactive fallouts as temporal makers for glacier ice cores dating. *The European Physical Journal Plus*, 127(6): 1-8.
- DEE D.P. (2011): The ERA-Interim reanalysis: configuration and performance of the data assimilation system. *Q.J.R. Meteorol. Soc.*, 137:553-597, April 2011 A.
- DELMONTE B, J.R. PETIT & V. MAGGI, 2002: Glacial to Holocene implications of the new 27000-year dust record from the EPICA Dome C (East Antarctica) ice core. *Climate Dynamics* 18: 647-660.
- DELMONTE B, BASILE-DOELSCH I, PETIT JR, MICHARD A, REVEL-ROLLAND M, MAGGI V, GEMMITI B, 2003: Refining the isotopic (Sr-Nd) signature of potential source areas for glacial dust in East Antarctica. *Journal de Physique IV*, 107: 365-368.
- MAGGI, V., VILLA, S., FINIZIO, A., DEL MONTE, B., CASATI, P., MARINO, F., 2004: Glaciers, climate change and anthropogenic impacts. Submitted to *Hydrobiologia*.
- General Assembly of the United Nation: Sustainable mountain development, *UN A/Res/62/196*, 2008.
- HAEBERLI W., HOELZLE M. (1995): Application of inventory data for estimating characteristics of and regional climate-change effects on mountain glaciers: a pilot study with the European Alps. *Annals of Glaciol.*, 21, 206–212.

- HAMMING R.W. (1986): Numerical Methods for Scientists and Engineers. *Unabridged Dover*, republication of the 2nd edition published by McGraw-Hill 1973.
- LINSBAUER A., PAUL F., HABERLI W. (2012): Modeling glacier thickness distribution and bed topography over entire mountain range with GlabTop: application of fast and robust approach. *Journal of Geo. Res.*, Vol. 117, F03007, 2012.
- OERLEMANS J (2001) *Glaciers and climate change. Balkema Publishers, Lisse.*
- OERLEMANS J. (2011) Minimal glacier models. *Second print. Igitur, Utrecht Publishing & Archiving Services, Universiteitsbibliotheek Utrecht.* ISBN 978-90-6701-022-1.
- ROGORA, M., MOSELLO, R. & MARCHETTO, A. Long-term trends in the chemistry of atmospheric deposition in Northwestern Italy: the role of increasing Saharan dust deposition. *Tellus B* **56**, 426–434 (2004).
- PATERSON, W. (1994), *The Physics of Glaciers, Pergamon, Tarrytown, N.Y.*
- PREUNKERT, S., D. WAGENBACH & M. LEGRAND, 2003: A seasonally resolved alpine ice core record of nitrate: comparison with anthropogenic inventories and estimation of preindustrial emissions of NO in Europe. *J. Geophys. Res.*, 108(D21), 4681, doi: 10.1029/2003JD003475.
- PREUNKERT S, M. LEGRAND & D. WAGENBACH, 2001. Sulfate trends in a Col du Dome (French Alps) ice core: A record of anthropogenic sulfate levels in the European midtroposphere over the twentieth century. *Journal of Geophysical Research-Atmospheres* 106 (D23): 31991-32004.
- PROSPERO J.M. & P.J.LAMB, 2004: African droughts and dust transport to the Caribbean: Climate change implications. *Science* : 1024-1027.
- PYE K., 1987: *Aeolian dust and dust deposits.* Academic Press, London, 245 pp.
- STEFFENSEN JP, 1997: The size distribution of microparticles from selected segments of the Greenland Ice Core Project ice core representing different climatic periods. *Journal of Geophysical Research-Oceans*, (C12): 26755-26763.
- TRETYAK and ZDESENKO 2002: *At. Data Nucl. Data Tables* 80, 83
- WAGENBACH, D, 1989: Environmental records in alpine glaciers, in *The Environmental Record in Glaciers and Ice Sheets*, pp. 69-83, J.Wiley and Sons, Chichester.
- WAGENBACH, D., S. PREUNKERT, J. SHAFER, W. JUNG and TOMADIN, 1996: Northward transport of Saharan dust recorded in a deep alpine ice core, in *The impact of desert dust across the Mediterranean*, pp. 291-300, Kluwer Academic Publisher, Dordrecht.
- ZANON G. (1982): Recent glaciological research in the Ortles- Cevedale region (Italian Alps). *Geogr. Fis. Din. Quat.*, 5(1), 75–81, 1982.